

# <sup>1</sup>H NMR Study of Molecular Motions in Thiourea Pyridinium Nitrate Inclusion Compound

M. Grottel<sup>a</sup>, A. Kozak, A. Pajzderska, W. Szczepański, and J. Wąsicki

Faculty of Physics, A. Mickiewicz University, 61-614 Poznań, Poland

<sup>a</sup> Department of Physics, Agricultural University, 60-637 Poznań, Poland

Reprint requests to Prof. J. W., Faculty of Physics, A. Mickiewicz University, ul. Umultowska 85, 61-614 Poznań, Poland

Z. Naturforsch. **59a**, 505 – 509 (2004); received April 6, 2004

The proton NMR second moment and spin-lattice relaxation time have been studied for polycrystalline thiourea pyridinium nitrate inclusion compound and its perdeuterated analogues in a wide temperature range. The reorientation of two dynamically different pyridinium cations around their pseudo-hexagonal symmetry axis taking place over inequivalent barriers have been revealed in the low-temperature phase. Activation parameters for these motions have been derived. A symmetrization of the potential barriers has been observed at the transition from intermediate to the high temperature phase. The motion of thiourea molecules has been also evidenced, but could not be unambiguously described.

**Key words:** NMR; Molecular Motion; Inclusion Compounds.

## 1. Introduction

Thiourea is well known to form crystalline inclusion compounds with a great variety of different guest molecules, like for example cyclohexane and its derivatives, organometallics and compounds containing aromatic rings [1–3]. The continued interest in such compounds lies in their usefulness as systems for molecular isolation and in the controlled, crystalline environments they represent for studies of molecular motions and interactions. Although there is a great number of such studies, many of the structural and dynamic properties of both host and guest molecules have not yet been well understood.

Our interest in the thiourea inclusion compounds has been focused on the molecular dynamics in such compounds with solid organic salts. Our previous NMR study of the thiourea pyridinium chloride, bromide and iodide inclusion compounds [4] has revealed in all the compounds a reorientation of the pyridinium cation over inequivalent barriers and hindered rotation of the thiourea molecule.

The present paper deals with an NMR study of the thiourea pyridinium nitrate inclusion compound  $[(\text{NH}_2)_2\text{CS}]_2(\text{C}_5\text{H}_5\text{NH})^+\text{NO}_3^-$  and its perdeuterated analogues  $[(\text{NH}_2)_2\text{CS}]_2(\text{C}_5\text{D}_5\text{NH})^+\text{NO}_3^-$  and  $[(\text{ND}_2)_2\text{CS}]_2(\text{C}_5\text{H}_5\text{ND})^+\text{NO}_3^-$ , hereafter denoted as

$\text{T}_2(\text{PyH})\text{NO}_3$ ,  $\text{T}_2(\text{d}_5\text{PyH})\text{NO}_3$  and  $\text{d}_8\text{T}_2(\text{PyD})\text{NO}_3$ , respectively. It was interesting to find out how the anion  $\text{NO}_3^-$  with its distinctly different shape from those of the halides affected the pyridinium reorientation.

Our DSC study of  $\text{T}_2(\text{PyH})\text{NO}_3$  has revealed two phase transitions: one at 216 K and another, first-order one, at 273 K on cooling and 281 K on heating.

Single crystal X-ray analyses made at 150 K, 250 K and 300 K have allowed to describe the molecular and crystal structure of the compound in its three phases [5]. The high-temperature (I) and intermediate (II) phases were found to be greatly disordered, while the low-temperature phase (III) is fully ordered with a network of strong hydrogen bonds. As in many other thiourea inclusion compounds [6], the orthorhombic structure observed for the high temperature phase (I) transforms to monoclinic structures of two other phases. Thus, the following sequence of phases has been found:  $\text{P}2_1 \rightarrow \text{P}2_1/c \rightarrow \text{P}bnm$ . The transition  $\text{II} \rightarrow \text{I}$  on heating is connected with parameter a double. In phase III two crystallographically inequivalent pyridinium cations have been revealed.

Hydrogen-bonded thiourea molecules form a channel parallel to the  $z$  axis and of a slightly distorted square cross section. In each channel there is a stack of pyridinium cations, the planes of which are inclined at an angle of about  $60^\circ$  to the channel axis.  $\text{NO}_3^-$  an-

ions are situated in the center of the distorted quadrilaterals.

## 2. Experimental

Stoichiometric amounts of thiourea and pyridinium nitrate were dissolved in a minimal quantity of boiling ethanol and left to cool. Crystals of thiourea pyridinium nitrate, twice recrystallized from ethanol, were then dried under vacuum. The perdeuterated analogue  $\text{T}_2(\text{d}_5\text{PyH})\text{NO}_3$  was prepared similarly, by a dissolution of stoichiometric quantities of thiourea and perdeuterated pyridinium nitrate ( $\text{C}_5\text{D}_5\text{NH})\text{NO}_3$ . To prepare  $\text{d}_8\text{T}_2(\text{PyD})\text{NO}_3$ , the thiourea was crystallized from  $\text{D}_2\text{O}$  to obtain perdeuterated thiourea  $(\text{ND}_2)_2\text{CS}$ , which was next dissolved with pyridinium nitrate in partially perdeuterated ethanol  $\text{C}_2\text{H}_5\text{OD}$ . All samples were ground to powder, degassed and sealed off under vacuum in glass ampoules.

The proton NMR spectra were recorded at a Larmor frequency of 28 MHz by using a home-made wide-line spectrometer. The second moment was calculated by numerical integration of the spectra and corrected for the finite modulation field. Measurements of the proton spin-lattice relaxation time  $T_1$  were made as a function of temperature with 58.9 and 25 MHz home-made pulse spectrometers, using the saturation recovery method. The temperature of the samples was controlled to an accuracy of 1 K.

## 3. Results

The temperature dependence of the proton NMR second moment obtained for  $\text{T}_2(\text{PyH})\text{NO}_3$  and its two perdeuterated analogues is presented in Figure 1. In phase III of  $\text{T}_2(\text{PyH})\text{NO}_3$  one observes a nearly constant  $M_2$  value of ca.  $13.8 \text{ G}^2$ , which diminishes in the phases II and I, reaching a quasi-plateau of  $4.5 \text{ G}^2$  at about 350 K. At the phase transition  $\text{II} \rightarrow \text{I}$  a jump of  $M_2$  is observed. For  $\text{T}_2(\text{d}_5\text{PyH})\text{NO}_3$  a constant value of the second moment of about  $15.4 \text{ G}^2$  is registered in phases III and II up to the temperature of the phase transition  $\text{II} \rightarrow \text{I}$ , where a jump-wise decrease of the second moment is observed. A further diminishing of the second moment in phase I leads to a plateau of  $6.2 \text{ G}^2$  registered at our high temperature limit.

For  $\text{T}_2(\text{d}_8\text{PyD})\text{NO}_3$  a monotonic decrease of the second moment from  $3.7 \text{ G}^2$  at 100 K to  $1.2 \text{ G}^2$  at 280 K is observed. Then, at the phase transition  $\text{II} \rightarrow \text{I}$

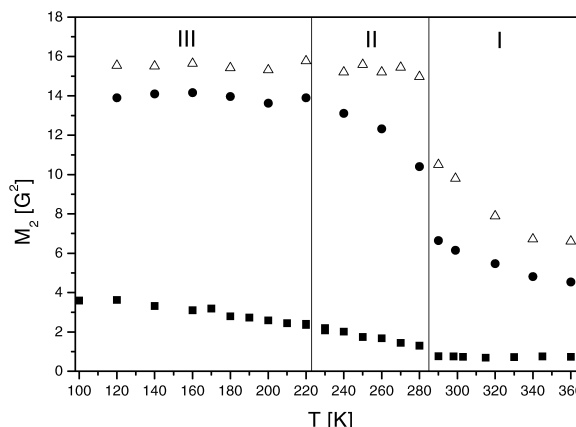


Fig. 1. Temperature dependences of the NMR second moment  $M_2$  of  $\text{T}_2(\text{PyH})\text{NO}_3$  (●),  $\text{T}_2(\text{d}_5\text{PyH})\text{NO}_3$  (△) and  $\text{d}_8\text{T}_2(\text{PyD})\text{NO}_3$  (■).

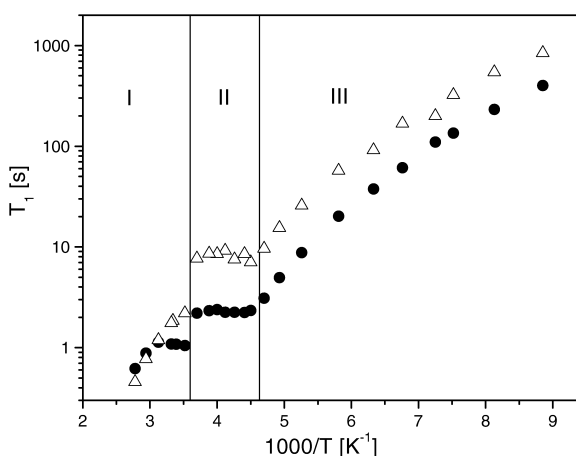


Fig. 2. Temperature dependences of the spin-lattice relaxation times  $T_1$  of  $\text{T}_2(\text{PyH})\text{NO}_3$  (●) and  $\text{T}_2(\text{d}_5\text{PyH})\text{NO}_3$  (△) at 58.9 MHz.

the second moment jumps to a plateau of  $0.75 \text{ G}^2$  in phase I.

The temperature dependence of  $T_1$  for  $\text{T}_2(\text{PyH})\text{NO}_3$  and  $\text{T}_2(\text{d}_5\text{PyH})\text{NO}_3$  is presented in Figure 2. The plots of the two samples are very similar, namely: a decrease of  $T_1$  is observed in phase III and nearly constant values in phase II. Then, in phase I, above the jump-wise decrease of  $T_1$  registered at the phase transition  $\text{II} \rightarrow \text{I}$  a further decrease of  $T_1$  is observed for  $\text{T}_2(\text{d}_5\text{PyH})\text{NO}_3$ , while for  $\text{T}_2(\text{PyH})\text{NO}_3$  a value of about 1.2 s is maintained up to ca 320 K, the temperature above which  $T_1$  starts to decrease again.

Figure 3 presents the temperature dependence of the spin-lattice relaxation time  $T_1$  obtained for  $\text{T}_2(\text{d}_8\text{PyD})\text{NO}_3$  at 58.9 MHz and 25 MHz. Both plots

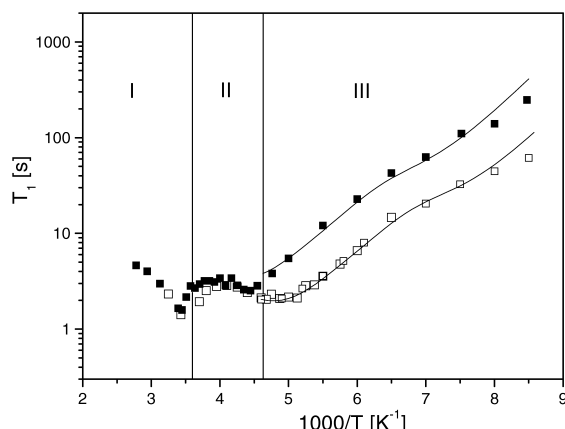


Fig. 3. Temperature dependences of the spin-lattice relaxation times  $T_1$  of  $\text{d}_8\text{T}_2(\text{PyD})\text{NO}_3$  at 25 MHz ( $\square$ ) and 58.9 MHz ( $\blacksquare$ ). The solid lines are theoretical fits to (3).

display a decrease of  $T_1$  in phase III, then a slight hill in phase II and an increase of  $T_1$  in phase I. The plot obtained for 25 MHz in phase III shows a wide  $T_1$  minimum of about 1.5 s.

#### 4. Calculation and Discussion

The proton second moments for the rigid structure of the compounds were found numerically by using the Van Vleck formula [7] and the X-ray data obtained in phase III. The lengths of the NH and CH bonds in the pyridinium cation and thiourea molecule were assumed to be 1.03 and 1.09 Å, respectively, as available from neutron diffraction data [8].

The values obtained: 13.8  $\text{G}^2$  for  $\text{T}_2(\text{PyH})\text{NO}_3$ , 15.9  $\text{G}^2$  for  $\text{T}_2(\text{d}_5\text{PyH})\text{NO}_3$  and 3.3  $\text{G}^2$  for  $\text{d}_8\text{T}_2(\text{PyD})\text{NO}_3$  correspond well to the respective experimental second moments observed in phase III, thus proving the rigidity of the pyridinium and thiourea sublattices at the low temperatures. The second moment calculation performed for the rigid structure of the two crystallographically different cations did not reveal any significant difference in the  $M_2$  values.

The reduction of the second moment observed at the higher temperatures reflects the onset of molecular reorientation in the crystal lattice. The question arises what type of reorientation it is. The values obtained at our high temperature limit indicate a complex motion of the molecules, that is: a reorientation of the pyridinium cation around the pseudohexagonal  $C'_6$  symmetry axis, followed by rotation of the thiourea molecule. The latter can not be precisely defined. It

can be a reorientation of  $\text{NH}_2$  groups around their  $n$ -fold axis ( $n \geq 3$ ) or a hindered rotation of the thiourea molecule around its C=S bond. The theoretical values obtained for both types of thiourea motion preceded by the cation reorientation are very similar and equal to about 4  $\text{G}^2$  for  $\text{T}_2(\text{PyH})\text{NO}_3$  and about 6  $\text{G}^2$  for  $\text{T}_2(\text{d}_5\text{PyH})\text{NO}_3$ , agreeing quite well with the experimental values obtained at the highest temperatures. Since the type of the thiourea motion can not be distinguished in our experiment, a further study of its dynamics is required. However, the occurrence of two motional processes ascribed to two dynamically different objects in the crystal lattice is well confirmed by the shape of the resonance line, showing two components of different linewidths.

The assumed model of pyridinium cation reorientation was confirmed in  $\text{T}_2(\text{d}_8\text{PyD})\text{NO}_3$ , in which the thiourea molecules were totally obscured by their full perdeuteration. The second moment, decreasing monotonically over a very wide temperature range (phases III and II), reflects the cation reorientation around its pseudo hexagonal  $C'_6$  axis, taking place between inequivalent potential wells, as was found in many other pyridinium salts [9–12]. At the phase transition  $\text{II} \rightarrow \text{I}$  one observes a jump-wise decrease to the plateau value of 0.75  $\text{G}^2$ , which can be ascribed to the cation reorientation over equivalent barriers in phase I. This means that at the phase transition there is a drastic change of the potential shape around the cation, leading to a symmetrization of the energy barriers. Such an effect was already observed in pyridinium nitrate and was supposed to trigger the solid-liquid phase transition [11].

To obtain activation parameters for the considered motion of the pyridinium cation, a model of six potential wells, five of equal depth and the sixth one evidently deeper, has been applied to calculate a theoretical spin-lattice relaxation time  $T_1$ . The assumed model of the potentials is well justified by the cation symmetry and our preliminary calculation of the energy barriers around the cation. The potential is characterized by two barriers of different heights, defined as activation energies  $E_A$  and  $E_B$ . In the model the time of the cation stay at the equilibrium position is assumed to be much longer than the time of a jump to the neighbouring equilibrium position. The value  $\Delta = E_A - E_B$  is a measure of the asymmetry of the potential barriers, while the population parameter is given by

$$a = \exp(-\Delta/RT). \quad (1)$$

The probability for transitions between two neighbouring wells is defined by

$$W_{BA} = K \exp(-E_B/RT), \quad (2)$$

where  $K$  is independent of temperature.

Then, the spin – lattice relaxation rate  $T_1^{-1}$  for the assumed model of the cation reorientation is given by the formula

$$\frac{1}{T_1} = \frac{8}{5} \gamma^2 \Delta M_2 \left[ \frac{2a}{1+5a} g(\tau_1) + \frac{3a}{(1+5a)^2} g(\tau_2) \right], \quad (3)$$

where

$$\tau_1 = \frac{1}{6W_{BA}},$$

$$\tau_2 = \frac{1}{(1+5a)W_{BA}},$$

$$g(\tau_i) = \frac{\tau_i}{1+\omega^2\tau_i^2} + \frac{4\tau_i}{1+4\omega^2\tau_i^2}.$$

$\Delta M_2$  is the change of the second moment due to the reorientation of the pyridinium cation between equivalent potential wells.

The reciprocal of the theoretical relaxation rate, calculated according to the (3) has been then fitted to the experimental  $T_1$  values obtained in phase III for  $d_8T_2(PyD)NO_3$  at the frequency of 58.9 and 25 MHz. This could not be done for one type of the pyridinium cation, so we had to assume two dynamically different cations, due to their crystallographical inequivalence. The input values of  $\Delta M_2$  were assumed to be the same for both cations and equal to  $1.5 \text{ G}^2$ . The sum of the reduction values ( $3 \text{ G}^2$ ) is well reflected in the  $M_2$  experiment performed for  $d_8T_2(PyD)NO_3$ , that is:  $3.7 \text{ G}^2$  (observed at the lowest temperatures) –  $0.75 \text{ G}^2$  (observed at phase I) =  $2.95 \text{ G}^2$ . Thus, the fitting procedure yielded activation parameters obtained in phase III for the reorientation of two dynamically different cations (Table 1). The extracted values characterising the unequal potential barriers are comparable with those obtained for the halides [4]. However, the existence of  $NO_3^-$  anions in the crystal lattice instead of the spherical halides is supposed to induce different crystalline environments of two cations, and in consequence their dynamical inequivalence.

The fitting procedure performed for  $d_8T_2(PyD)NO_3$  in phase I has yielded the activation energy  $12 \text{ kJ/mol}$ ,

Table 1. The fitted activation parameters and  $\Delta M_2$  values of  $d_8T_2(PyD)NO_3$  (phase III) for the  $C'_6$  reorientation over inequivalent potential barriers of two dynamically different pyridinium cations.

	Cation 1	Cation 2
$E_A$ [kJ/mol]	22.5	18.8
$E_B$ [kJ/mol]	14.8	10.5
$K$ [s <sup>-1</sup> ]	$1.98 \cdot 10^{12}$	$4.82 \cdot 10^{12}$
$\Delta M_2$ [G <sup>2</sup> ]	1.5	1.5

which characterizes the cation reorientation over symmetrical barriers in that phase, as revealed in the second moment experiment.

The relaxation plots observed at the intermediate phase II probably result from an overlap of two relaxation processes, e.g. the pyridinium cation reorientation and a slower motion of the thiourea molecules. However, one can not exclude the existence of an incommensurate phase, caused by coulombic interactions in the compound [13].

The thiourea reorientation starts to affect strongly the relaxation only in phase I, which is manifested by the shortening of the  $T_1$  values observed in  $T_2(PyH)NO_3$  and  $T_2(d_5PyH)NO_3$ . Unfortunately, the limited experimental data did not allow to extract the activation parameters for this motion.

Worth noting are abrupt changes in all parameters measured at the phase transition II → I pointing to order-disorder character of the transition. Besides the drastic changes of the crystallographical parameters, jump-wise changes in the relaxation time and second moment have also been observed. It thus provides an evidence that the structure transformation is accompanied by drastic changes in the molecular dynamics of the compound. The symmetrization of the energy barrier for the pyridinium cation reorientation, revealed in the second moment experiment, could be a mechanism triggering the phase transition II → I, as was observed in the pyridinium nitrate.

## 5. Conclusions

An <sup>1</sup>H NMR study performed for thiourea pyridinium nitrate inclusion compounds has revealed a complex molecular motion, that is: a reorientation of two dynamically different pyridinium cations around a pseudohexagonal symmetry axis taking place over inequivalent barriers, followed by a reorientation of the thiourea molecule the nature of which could not be distinctly described. The activation parameters de-

rived for the cation reorientation in phase III are comparable to those found for previously studied halides. The occurrence of  $\text{NO}_3^-$  anions in the crystal lattice are supposed to induce crystallographical and dynamical inequivalence of the pyridinium cations. The drastic change in the molecular dynamics observed at the phase transition, leading to a symmetrization of the

energy barriers for the cation reorientation, can be a mechanism triggering the phase transition.

#### Acknowledgement

The authors thank Dr. S. Mielcarek for the DSC study and Dr. S. Lewicki for his assistance in performing the  $T_1$  measurements at 25 MHz.

- [1] A. Desmedt, S. J. Kitchin, F. Guillaume, K. D. M. Harris, and E. H. Bocanegra, *Phys. Rev. B* **64**, 054106 (2001).
- [2] Chi-Keung Lam and T. C. W. Mak, *Tetrahedron* **56**, 6657 (2000).
- [3] K. D. M. Harris, *J. Mol. Structure* **374**, 241 (1996).
- [4] M. Grottel, A. Pajzderska, and J. Wąsicki, *Z. Naturforsch.* **58a**, 638 (2003)
- [5] P. Czarnecki and H. Małuszyńska, to be published.
- [6] M. D. Hollingsworth and K. D. M. Harris, *Comprehensive Supramolecular Chemistry*, Vol. 6, Pergamon, Oxford 1996.
- [7] J. H. van Vleck, *Phys. Rev.* **74**, 1168 (1948).
- [8] G. R. Desiraju and T. Steiner, *The Weak Hydrogen Bond*, Oxford University Press, 2001.
- [9] J. A. Ripmeester, *J. Chem. Phys.* **85**, 747 (1986).
- [10] Y. Ito, T. Asaji, R. Ikeda, and D. Nakamura, *Ber. Bunsenges. Phys. Chem.* **92**, 885 (1988).
- [11] A. Kozak, M. Grottel, J. Wąsicki, and Z. Pająk, *Phys. Stat. Sol.* **143a**, 65 (1994).
- [12] M. Grottel and R. Jakubas, *Solid State Comm.* **111**, 29 (1999).
- [13] A. Janner, T. Janssen, and P. M. de Wolff, *Europhysics News* **13**, 12 (1982).